Broadband Infrared Transmission in a Hollow-Core Photonic Bandgap Fibre Free of Surface Modes.

R. Amezcua-Correa (1), M.N. Petrovich (1), N. G. Broderick (1), D.J. Richardson (1),
T. Delmonte (2), M.A. Watson (2), E.J. O'Driscoll (2)
(1) Optoelectronics Research Centre (ORC), University of Southampton, Southampton SO17 1BJ, UK.
(2) BAE SYSTEMS Advanced Technology Centre, Sowerby Building, Filton, Bristol, BS34 7QW, UK
E-mail: rac@orc.soton.ac.uk

Abstract *We report low-loss, wide bandwidth short wavelength infrared guidance in a hollow-core silica photonic bandgap fibre free of surface modes. The bandgap's centre is around 2μm with a 3dB bandwidth of* approximately *350nm.*

Introduction

Hollow-core photonic bandgap fibres (PBGFs) confine light within an air-core due to photonic bandgap effects. Such fibres allow for a very weak overlap between the guided mode and the fibre structure, which paves the way for novel and technologically enabling properties, such as low nonlinearity, high damage thresholds and transmission beyond silica's own transparency window [1]. Mid-IR transmission, not feasible in conventional fibres due to the very high absorption of silica beyond 2μm [2], has been recently demonstrated in silica PBGFs [3,4]. However, these fibres had a narrow low-loss operational bandwidth of less than 100nm, due the presence of surface modes (SMs) at their core-cladding interfaces [5]. Recently, we have identified optimum fibre design regimes that maximize the wavelength range for which the "fundamental" air-guided mode (FM) is free of anticrossings with surface modes [6]. In this paper, we report on the fabrication and characterization of a PBGF with a wide bandgap centred at about 2μm and free of SMs.

Fibre design

We modelled an idealized but realistic representation of a 7-cell core, high air-filling fraction PBGF. The cladding holes were represented by hexagons with rounded corners described by the relative hole diameter, d/Λ, and the relative radius of curvature at the corners, D_C/Λ [7]. The core is defined by a thin non-circular silica ring of nearly constant thickness T_C at the boundary with the cladding as shown in Fig.1. A normalised core boundary thickness was defined by dividing T_C by the thickness of the struts in the cladding, i.e. $T = T_C/(\Lambda - d)$. In this study we assumed $d/\Lambda = 0.95$ and $D_C/\Lambda = 0.55$, which we believe were realistic targets for fabrication, and also chose a pitch of $\Lambda = 4.3\mu m$, which resulted in a PBGF with bandgap centred at 2μm.

A systematic investigation of the effect of the ring thickness on the fibre's transmission properties was carried out. The normalized boundary thickness (T) was varied in the range $0.175 \le T \le 3.5$ and for each fibre we solved for the modes within the bandgap [6]. In order to assess the performance of the various structures we calculated the normalized interface field intensity of the fundamental air-guided mode, factor F [8]. This factor suffices to identify designs with broad transmission spectra as its value critically depends on whether or not the fibre supports surface modes [6,8].

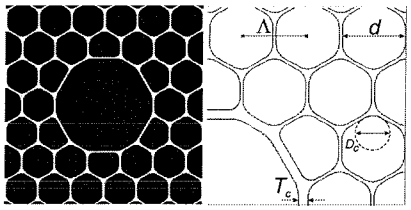

Fig. 1 *Cross section of a modelled PBGF and the parameters used to define the structure.*

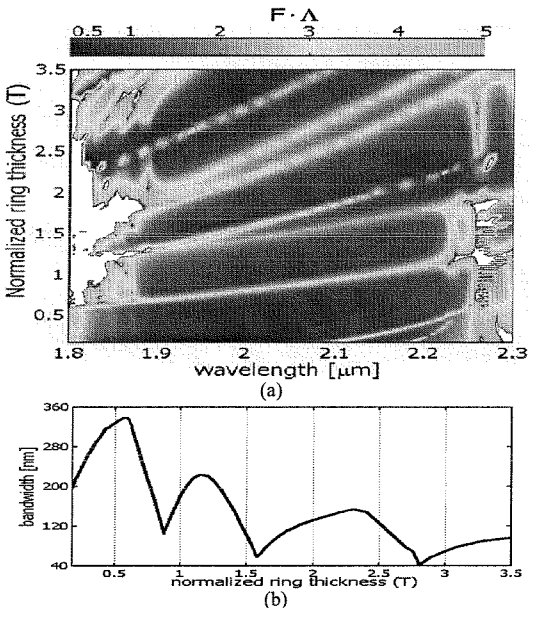

Fig. 2 *(a) Normalized interface field intensity F vs. wavelength and normalized ring thickness. (b) Bandwidth of transmission vs normalised thickness for PBGFs operating at $\lambda = 2\mu m$.*

Figure 2(a) shows the calculated factor F as a function of T and of the wavelength. In this design map, $F\Lambda \le 1$ (blue) denote regions where the FM is tightly confined in the core, and light cyan diagonal lines ($F\Lambda \approx 3$) correspond to anticrossing points between the fundamental core mode and SMs (note that some lines appear not continuous in the graph due to the discrete number of the T values considered); $F\Lambda \approx 4$ (green) correspond to wavelengths at which the FM is outside the gap, i.e. it coexists with cladding modes; finally, white represents regions where an air guided FM is no longer supported. From the map, we can immediately

see that the fibre with a core boundary thickness of T=0.175 (the lowest value assumed in this study) supports two SMs that interact with the fundamental mode at about 2.1 and 2.2μm. However, by increasing the ring thickness, the anticrossing points move towards the long wavelength edge of the gap, and the operational bandwidth of the fibre is correspondingly increased. The FM of the fibre with T≈0.6 is free of anticrossing for all wavelengths within the gap, as is also shown in the modal dispersion curve in Fig. 3(a) (the shaded region denotes the bandgap). A further increase of the core ring thickness causes a new SM to appear close to the short wavelength edge and again the bandwidth is reduced.

For each fibre design, we have estimated the operational bandwidth by setting a threshold value for $F\Lambda \leq 1$. The plots in Fig. 3 show that this assumption is reasonable, since $F\Lambda$ is approximately equal to one at wavelengths where the FM crosses the bandgap edges. The results are presented in Fig.2(b) clearly showing that PBGF structures with rings of thickness in the range $0.45 \leq T \leq 0.65$ are optimal for broadband transmission, providing a maximum operating bandwidth of ≈350nm at λ=2μm for T=0.575.

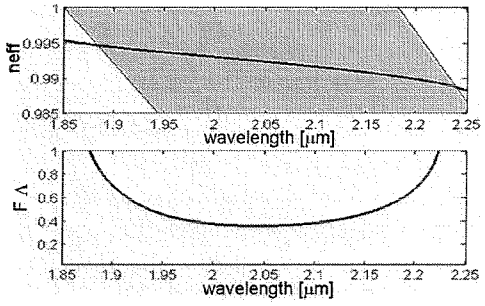

Fig. 3 *Calculated (a) Effective index of modes vs. λ (b) normalized field intensity vs. λ for a fibre with an optimum core surround thickness T=0.6.*

Fibre Fabrication and measurements

Fabrication of a PBGF with the designed optimum structure was undertaken. Detailed structural analysis was performed by scanning electron microscopy (SEM), which allowed us to verify that the thickness of the silica ring was within the regime for wide bandwidth operation (Fig. 4). The fibre has a 7-cell core and seven rings of holes surrounding it, plus one incomplete ring to facilitate stacking and structural integrity during fibre fabrication. The air filling factor of the cladding is ≈ 89% and the pitch is about the same value (4.3μm) as assumed in our modelling study.

The fibre transmission was measured using an OPO source, which could be continuously wavelength-tuned across the bandgap. Figure 5 shows a plot of the total loss (fibre loss plus coupling loss) vs. the wavelength. Fibres lengths of 6m and 1m were used for the measurements. Little variation in the fibre transmission at the centre of the bandgap was observed between samples with different lengths, which indicates low fibre loss and good structural uniformity. Light transmitted at 2μm showed good beam quality (M^2≈1.4).

The fibre showed a wide, low loss region completely free of surface modes; from the data shown in Fig.5, we estimated an operational bandwidth spanning approximately 350nm for a fibre operating at ≈2 μm. This result is in very good agreement with the predictions of modelling shown in Fig. 3.

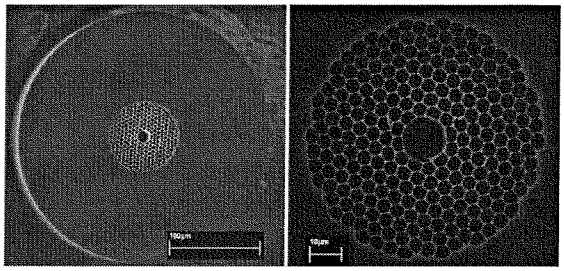

Fig. 4 *Cross-sectional SEM images of the fibre designed to operate at 2μm.*

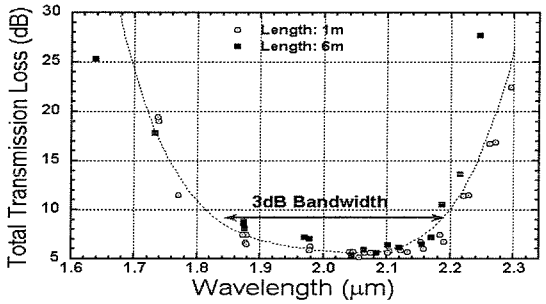

Fig. 5 *Bandwidth of transmission of the PBGF designed for operation at 2μm.*

Conclusions

We have demonstrated a high air filling fraction silica PBGFs with an optimized core design achieving a wide transmission spectrum of $\approx 350nm$ centred at $\approx 2\mu m$. The fundamental air-guided mode of the manufactured fibre is not affected by surface modes at any wavelengths within the bandgap. The measured operational bandwidth is in very good agreement with the predictions of our modelling for the measured fibre structural parameters.

Acknowledgements

This work was partly funded by the Electro-Magnetic Remote Sensing (EMRS) Defence Technology Centre, established by the UK Ministry of Defence.

References

1 P. Russell, Science, **299** (2003), 358.

2 O. Humbach, et al., J. Non-cryst. Solids, **203** (1996), 19.

3 J. D. Shephard, et al., Opt. Express, **13** (2005), 7139.

4 T. J. Stephens, et al., Proc. CLEO (2004), paper CPDD4.

5 J. West, et al., Opt. Express, **12** (2004), 1485.

6 R. Amezcua-Correa, et al., Proc. OFC (2006), paper OFC1.

7 N.A. Mortensen, et al., Opt. Lett., **29** (2004), 349.

8 P. J. Roberts, et al., Opt.. Express, **13** (2005),8277.